Surface & Coatings Technology 232 (2013) 290–297

Contents lists available at ScienceDirect

Surface & Coatings Technology

journal homepage: www.elsevier.com/locate/surfcoat

# Numerical investigations on the effect of total pressure and nozzle divergent length on the flow character and particle impact velocity in cold spraying

Shuo Yin [a,b,*], Meng Zhang [a], Zhiwei Guo [c,b], Hanlin Liao [b], Xiaofang Wang [a]

[a] *School of Energy and Power Engineering, Dalian University of Technology, Dalian 116024, Liaoning, China*
[b] *LERMPS (Laboratoire d'Etudes et de Recherches sur les Matériaux, les Procédés et les Surfaces), Université de Technologie de Belfort-Montbéliard, Site de Sévenans 90010, Belfort Cedex, France*
[c] *School of Water Resources and Hydropower Engineering, Wuhan University, Wuhan 430027, Hubei, China*

## ARTICLE INFO

*Article history:*
Received 5 February 2013
Accepted in revised form 14 May 2013
Available online 21 May 2013

*Keywords:*
Cold spraying
Computational fluid dynamics (CFD)
Numerical simulation
Impact velocity
Total pressure
Divergent length

## ABSTRACT

This study investigates the effect of total pressure ($P_0$) and nozzle divergent length ($L_d$) on the flow character and particle impact velocity in cold spraying. Computational fluid dynamic (CFD) approach is employed in the present work to achieve this objective. The simulated results indicate that $P_0$ and $L_d$ significantly influence the flow regime and particle acceleration. With gradually increasing $P_0$, the nozzle exit Mach number ($M_e$) firstly increases and then fluctuates after $P_0$ exceeds a critical value, finally $M_e$ reaches the maximum value and maintains stable. Differing from $M_e$, the particle impact velocity ($V_p$) continually goes up with $P_0$ due to the increasing gas density which can improve the drag force, but the growth rate levels out gradually. Besides, it is also found that $M_e$ shows a downward trend with increasing $L_d$. However, as for $V_p$, there exists an optimal $L_d$ which can guarantee the particle achieving the maximum $V_p$. Moreover, for nozzles with larger expansion ratio, the optimal $L_d$ is longer. This optimal length is considered as a consequence of the competition between the particle acceleration time and drag force on the particle surface.

## 1. Introduction

Cold spraying (CS) is a relatively new coating technique developed in the mid-1980s and has been rapidly developing during the past two decades. In this process, powder particles (typically <50 μm) are accelerated to a high velocity ranging from 300 to 1200 m/s by a supersonic gas flow and then impinging onto a substrate in solid state without significant fusion, undergoing intensive plastic deformation. The 'low temperature' in CS process can minimize the adverse effect brought by molten or semi-molten state, providing a possibility to coat oxygen-sensitive materials [1,2]. Generally, particle velocity prior to the impact is an important factor that determines whether particles can adhere on the substrate surface. It has been widely accepted that there exists a material-dependent critical velocity for a given condition (e.g. specific particle size, temperature and material properties), only above which bonding at the particle/substrate interface can take place and the CS coating can be formed on the substrate surface [3–7]. As for the bonding mechanism, the most acceptable view can be regarded as the occurrence of adiabatic shear instability (ASI) at the interface. At the region where ASI occurs, thermal softening is dominant over work hardening, resulting in the forming of outward metal jet. Such viscous-like metal jet helps to clean up the oxide film which originally exists on the particle and substrate surfaces, allowing the metallic bonding to occur [3,4].

It is known that CS particles are dragged and accelerated by the compressed carrier gas. The particle in-flight velocity is highly dependent on the character of the gas flow inside and outside the nozzle. As for the gas flow regime, it is influenced by several factors, including operating parameters, nozzle geometry and standoff distance, etc. Therefore, it is necessary to adjust these influencing factors in order to obtain an optimal flow regime which can guarantee the particles achieving the highest impact velocity. Experimental observation on the gas flow inside and outside the nozzle should be the best way to well understand the flow regime and particle acceleration in CS. However, this is a money- and time-consuming work, which is rather difficult to be carried out. In the last decades, computational fluid dynamics (CFD) technique is making increasingly important contributions to predict the gas flow regime and particle velocity in CS due to its less economic and time consumption than experimental implementations [8–16]. Among these studies, sizable works concentrated on the optimization of nozzle geometry for achieving the optimal supersonic gas flow regime and hence maximizing the particle impact velocity [8–13]. It has been found that there exists an optimal expansion ratio for a given operating condition. The nozzle with an optimal expansion ratio can significantly reduce the shockwaves outside the nozzle and maximize the particle kinetic energy [8–10]. Nozzle cross-section shape also influences the particle velocity and

---

* Corresponding author at: School of Energy and Power Engineering, Dalian University of Technology, Dalian, Liaoning 116024, P.R. China. Tel./fax: +86 411 84707905.
*E-mail address:* s.yin1984@hotmail.com (S. Yin).

0257-8972/$ – see front matter © 2013 Elsevier B.V. All rights reserved.
http://dx.doi.org/10.1016/j.surfcoat.2013.05.017

dispersion. Circular and square cross-sections result in higher particle velocity while elliptical cross-section makes the particles more dispersed [11–13]. On the other hand, the optimization of operating parameters, such as inlet pressure, inlet temperature, gas type and standoff distance is another focus. [9,10,14–16]. The research results indicate that increasing the inlet pressure, temperature or using Helium as the carrier gas can increase the particle impact velocity. In the current work, total pressure ($P_0$) and nozzle divergent length ($L_d$) are selected as two key concerns. A detailed investigation on these two factors is performed by CFD method to clarify their effects on the flow regime, nozzle exit Mach number ($M_e$) and particle impact velocity ($V_p$). In addition, one-dimensional (1D) isotropic flow is also solved and compared with the two-dimensional (2D) full Navier–Stokes solution to evaluate the possible velocity loss during the gas expansion process inside the nozzle.

## 2. Numerical methodology

### 2.1. Computational domain and boundary conditions

Numerical simulations are performed by using ANSYS-FLUENT 12.1 to predict the gas flow regime and particle velocity in CS [17]. The 2D axi-symmetric model is used to limit the computational resources. The de-Laval nozzles used in this study have a circular cross-section with an inlet diameter of 17 mm. Compressed carrier gas expands from the throat with a fixed diameter of 2.2 mm to the nozzle outlet. Three expansion ratios, namely, 4.0, 8.0 and 12.0, are considered and the corresponding exit diameters are 4.4, 6.22 and 7.62 mm, respectively. The convergent section has a length of 30 mm, which is attached to the throat directly. $L_d$ is varied from 80 to 440 mm. The flat substrate is a circular plate with the diameter of 60 mm and located 30 mm away from the nozzle exit. The outer boundary of the computational domain of the impinging jet is extended 20 mm away from the substrate back and edge. Fig. 1 shows the computational domain and boundary conditions of the numerical model. The computational domain is meshed into a number of quadrilateral cells and the total number of the grid cells varies from 10,984 to 38,648, depending on the expansion ratio and $L_d$. The grid at the nozzle throat region and impinging jet region is refined to accurately capture the rapid variation of flow properties due to the highly compressible character of the supersonic carrier gas. The grid independent test confirms that such amount is sufficient to guarantee a grid-independent solution. The local computational grid is illustrated in Fig. 2. The gas inlet is treated as the pressure inlet with the total temperature ($T_0$) of 600 K and $P_0$ of 0.5 ~ 4.0 MPa. The pressure-far-field boundary is applied to the surrounding atmosphere. The outlet of the computational domain is modeled using the pressure outlet with the pressure of 0.1 MPa. Standard non-slip condition is used to the substrate surface and nozzle wall which are assumed to be insulated. The mathematic description of the boundary conditions is listed in Table 1, where $R_\infty$ and $R_i$ are Riemann invariants, $v_n$ is the velocity magnitude normal to the boundary. The detailed description on the boundary conditions, especially the pressure-far-field boundary can be referred in Ref. [17].

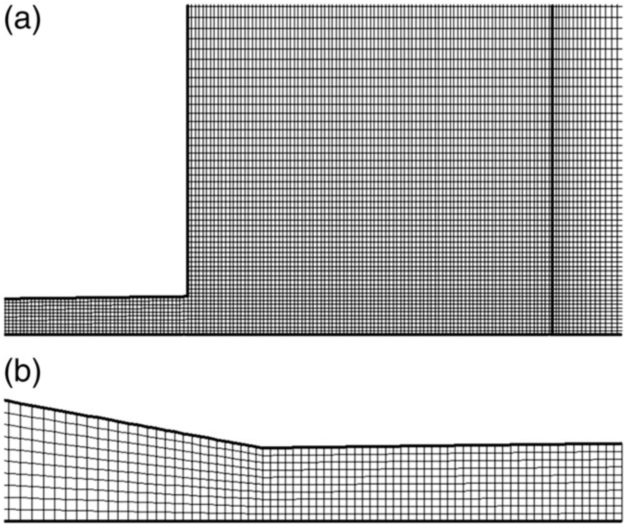

**Fig. 2.** Local grid at the nozzle throat region (a) and free jet region (b).

### 2.2. Gas phase and solid phase

Air is chosen as the carrier gas and the gas properties are listed in Table 2. The ideal gas law is used to calculate the density in order to take the compressibility effects into consideration. The governing equations for a 2D steady compressible flow in the rotating coordinate system can be written as follows:

Continuity equation:

$$\frac{\partial}{\partial z}(\rho u_z)+\frac{1}{r}\frac{\partial}{\partial r}(\rho r u_r)=0 \tag{1}$$

$z$-momentum equation:

$$\frac{\partial \rho u_z u_r}{\partial z}+\frac{1}{r}\frac{\partial \rho r u_z u_r}{\partial r}=-\frac{\partial P}{\partial z}+2\frac{\partial}{\partial z}\left(\mu\frac{\partial u_z}{\partial z}\right)+\frac{1}{r}\frac{\partial}{\partial r}\left[\mu r\left(\frac{\partial u_z}{\partial r}+\frac{\partial u_r}{\partial z}\right)\right] \tag{2}$$

$r$-momentum equation:

$$\begin{aligned}\frac{\partial \rho u_z u_r}{\partial z}+\frac{1}{r}\frac{\partial \rho r u_r u_r}{\partial r}=&-\frac{\partial P}{\partial z}+\frac{2}{r}\frac{\partial}{\partial r}\left(\mu r\frac{\partial u_r}{\partial r}\right)\\&+\frac{\partial}{\partial z}\left[\mu\left(\frac{\partial u_z}{\partial r}+\frac{\partial u_r}{\partial z}\right)\right]-\frac{2\mu u_r}{r^2}\end{aligned} \tag{3}$$

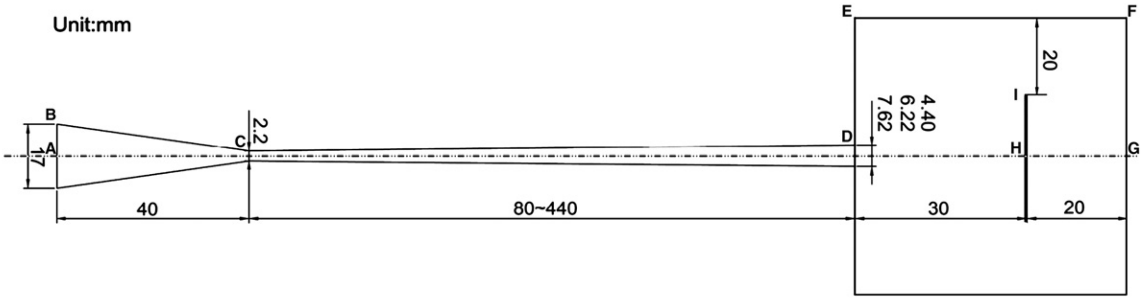

**Fig. 1.** Computational domain and boundary conditions.